
Electronic Thesis and Dissertation Repository

8-26-2024 5:30 PM

Stability of long multiple-rod constructs and dual-rod constructs in the thoracic spine: a biomechanical cadaveric study

Brandon J. Herrington, *Western University*

Supervisor: Rodrigues Fernandes, Renan, *The University of Western Ontario*

Co-Supervisor: Rasoulinejad, Parham, *The University of Western Ontario*

Co-Supervisor: Bailey, Chris, *The University of Western Ontario*

A thesis submitted in partial fulfillment of the requirements for the Master of Science degree in Surgery

© Brandon J. Herrington 2024

Follow this and additional works at: <https://ir.lib.uwo.ca/etd>



Part of the [Orthopedics Commons](#)



This work is licensed under a [Creative Commons Attribution-Noncommercial 4.0 License](#)

Recommended Citation

Herrington, Brandon J., "Stability of long multiple-rod constructs and dual-rod constructs in the thoracic spine: a biomechanical cadaveric study" (2024). *Electronic Thesis and Dissertation Repository*. 10394. <https://ir.lib.uwo.ca/etd/10394>

This Dissertation/Thesis is brought to you for free and open access by Scholarship@Western. It has been accepted for inclusion in Electronic Thesis and Dissertation Repository by an authorized administrator of Scholarship@Western. For more information, please contact wlsadmin@uwo.ca.

ABSTRACT

Spinal fusion to correct spinal deformity is typically performed with a 2-rod construct spanning the targeted area of fusion. More evidence is starting to emerge around the utility of multiple-rod constructs (typically 3 or more rods) to increase the stiffness and stability of a spinal fusion construct. Much of this work has focused on the lumbar spine, and little has been published around how these constructs behave in a long construct spanning the thoracic spine. The purpose of this thesis is to compare the stability of a two-rod (dual-rod) construct (DRC) to a four-rod (multiple-rod) construct (MRC) in cadaveric thoracic spines. Nine intact human cadaveric thoracic spines (T1-T12) were instrumented with either a DRC or MRC, and biomechanical testing was then carried out to compare range of motion (ROM) and stiffness between these two constructs. Results demonstrated comparable absolute total ROM and stiffness between DRCs and MRCs, and this was consistent across all measured vertebral levels. However, after undergoing a 1-hour bodyweight simulation fatigue test, DRCs exhibited an increase in flexion/extension ROM and decrease in stiffness while MRCs did not. Overall, these findings support previous clinical and biomechanical results in the lumbar spine and adult spinal deformity literature that MRCs can potentially be used to increase the stability of thoracic spine constructs.

KEYWORDS

Cadaver, Spinal Fusion, Thoracic Spine, Adult Spinal Deformity, Two-Rod Construct, Dual-Rod Construct, Satellite Rod, Multiple-Rod Construct, Proximal Junctional Kyphosis

SUMMARY FOR LAY AUDIENCE

Spinal fusion, where two or more segments of the spine are fused together, is a common method to treat various types of spinal pathology. In order to accomplish a successful spinal fusion, the amount of motion at the fusion site must be decreased to a certain level to allow adequate bone formation across the segment. To decrease the amount of motion at a fusion site, the spine is instrumented at each level with screws and rods. Typically, two rods are used in a construct (one on each side), with two screws at each vertebral level. However, sometimes this two-rod construct is not rigid enough and excessive motion at the fusion site persists.

When too much motion occurs at the attempted fusion site, instead of bone forming across the fusion site, the area is filled with stable scar or fibrous tissue—this is called a nonunion or pseudarthrosis. Nonunion can lead to ongoing pain and increased motion that leads to continued stress on implants. As the implants are subjected to ongoing stress, complications can occur, such as the screws pulling out from the bone, or the rods themselves breaking. When instrumentation fails, this can then lead to further progression of deformity, pain, and even neurologic deficits, ultimately resulting in the need for additional surgery.

In an attempt to increase stability at the surgery site and to prevent nonunion, many deformity surgeons have started to use three or more rods (multiple-rod constructs) to augment instrumentation. This has had promising results in the biomechanical and clinical literature within the lumbar spine, but biomechanical research is lacking on how these constructs behave in the thoracic spine. In this thesis, two different types of instrumentation methods—a dual-rod construct and multiple-rod construct—in the thoracic spines of cadavers were compared.

Overall, dual-rod constructs and multiple-rod constructs exhibited similar absolute stability. But when each construct was subjected to 1 hour of simulated day-to-day wear and tear, multiple-rod constructs appeared more resistant to change in stiffness and range of motion. This supports the idea that multiple-rod constructs provide additional stability in the initial phase immediately after surgery, when bone is attempting to fuse. This has important consequences as multiple-rod constructs can be used to increase construct stiffness, which can potentially result in less nonunion and reduce the incidence of revision surgery after spinal fusion, ultimately leading to improved patient satisfaction and outcomes.

CONTRIBUTIONS

Multiple team members were involved in the generation of this thesis, each with their own expertise. These contributions are as follows:

Chapter 1: Brandon Herrington – sole author

Chapter 2: Brandon Herrington – study design, cadaveric preparation, data collection, data analysis, manuscript writing; Chloe Cadieux – cadaveric preparation, data collection; Pawel Brzozwski – study design, data collection, data analysis; Parham Rasoulinejad – reviewed manuscript; Chris Bailey – reviewed manuscript; Renan Rodrigues Fernandes – study design, reviewed data analysis, reviewed manuscript.

Chapter 3: Brandon Herrington – study design, data collection, data analysis, manuscript writing; Pawel Brzozwski – study design, data collection, data analysis; Parham Rasoulinejad – reviewed manuscript; Chris Bailey – reviewed manuscript; Renan Rodrigues Fernandes – study design, reviewed data analysis, reviewed manuscript.

Chapter 4: Brandon Herrington – sole author.

ACKNOWLEDGEMENTS

Thank you to my supervisor Dr. Renan Rodrigues Fernandes for supporting me in this opportunity to pursue this project as part of my Master's degree. I'm deeply appreciative of his patience and expertise throughout this project. He, as well as my co-supervisors Dr. Rasoulinejad and Dr. Bailey, have not only helped guide me through this endeavor, but also provided me with exceptional mentorship throughout my Orthopaedic Surgery residency.

My gratitude goes to Pawel Brzozowski for all of the countless hours he spent in the lab running tests, as well as behind the scenes extracting data and running analyses.

A special thank you is extended to the DePuy Synthes organization for kindly donating the required hardware and materials to pursue this thesis.

I would also like to thank all of those who donated their bodies to science, as well as their families. This project would not be possible without this selfless gesture.

TABLE OF CONTENTS

ABSTRACT.....	ii
KEYWORDS.....	iii
SUMMARY FOR LAY AUDIENCE.....	iv
CONTRIBUTIONS	vi
ACKNOWLEDGEMENTS.....	vii
TABLE OF CONTENTS	viii
LIST OF TABLES	x
LIST OF FIGURES	xi
CHAPTER 1	1
1 – INTRODUCTION	1
1.1 – ANATOMY OVERVIEW	1
1.2 – PSEUDARTHROSIS AND IMPLANT-RELATED COMPLICATIONS.....	6
1.3 – INCREASING ROD STIFFNESS.....	8
1.3.1 – ROD MATERIAL.....	8
1.3.2 – ROD DIAMETER	9
1.3.3 – ROD SHAPE	9
1.3.4 – NUMBER OF RODS.....	10
1.4 – THESIS RATIONALE.....	12
CHAPTER 2	13
2 – METHODS	13
2.1 – CADAVER PREPARATION.....	13
2.2 – INSTRUMENTATION	16
2.3 – SPECIMEN TESTING	20
2.4 – STATISTICAL ANALYSIS.....	24
CHAPTER 3	25
3 – RESULTS.....	25
3.1 – TOTAL RANGE OF MOTION AND STIFFNESS	25
3.1.1 – ROTATION.....	27
3.1.2 – LATERAL BEND.....	27
3.1.3 – FLEXION/EXTENSION.....	27
3.2 – RANGE OF MOTION BY VERTEBRAL SEGMENT	29

3.2.1 – ROTATION BY VERTEBRAL SEGMENT	31
3.2.2 – LATERAL BEND BY VERTEBRAL SEGMENT.....	33
3.2.3 – FLEXION/EXTENSION BY VERTEBRAL SEGMENT	35
CHAPTER 4	37
4 – DISCUSSION.....	37
4.1 – DISCUSSION AND SUMMARY	37
4.2 – LIMITATIONS.....	41
4.3 – CONCLUSION.....	43
REFERENCES	44

LIST OF TABLES

Table 1: Demographics of cadaveric specimens	14
Table 2: Total range of motion and stiffness, comparison by fatigue status	29
Table 3: Total range of motion and stiffness, comparison by construct type	29
Table 4: Range of motion by vertebral segment	31

LIST OF FIGURES

Figure 1: Anatomy of the vertebral column	3
Figure 2: Anatomy of the thoracic vertebra	4
Figure 3: Apophyseal joint orientation variation	5
Figure 4: Cadaveric specimen preparation.....	15
Figure 5: Instrumentation of dual-rod and multiple-rod constructs	18
Figure 6: Attachment of markers for digital image correlation system	19
Figure 7: Biomechanical testing set-up	23
Figure 8: Graphical comparison of total range of motion	27
Figure 9: Rotation by vertebral segment	3
Figure 10: Lateral bend by vertebral segment	35
Figure 11: Flexion/extension by vertebral segment	37

CHAPTER 1

1 – INTRODUCTION

This chapter provides an overview into relevant spine anatomy, background on various methods to increase stability in spine surgery, as well as a literature review of the current evidence around multiple-rod and dual-rod constructs.

1.1 – ANATOMY OVERVIEW

The vertebral column extends from the skull, down to the middle of the buttocks where it articulates with the right and left innominate bones of the pelvis girdle. In total, it makes up about two fifths of the total height of the human body. This column is composed of 33 total vertebrae divided into 5 distinct regions—7 cervical, 12 thoracic, 5 lumbar, 5 sacral, and 4 coccygeal (Figure 1). These individual vertebrae can move relative to each other, and together, they form the central weight-bearing axis of the body, support the head, and transfer weight to the abdomen and legs. The complex interaction between the vertebrae, muscles, and ligaments allows for multidirectional movement, and protection of the spinal neural elements¹.

Overall, except for the first and second cervical vertebrae, the individual vertebrae of the spine share many common features. They consist of a vertebral body anteriorly, the vertebral arch, and four articular processes—2 superior and 2 inferior—that connect vertebrae to each other. The vertebral body is anterior and bears much of the weight of an individual. The vertebral arch travels posteriorly from the body and is made up of the pedicles and bilateral laminae, which then connect to the transverse and spinous processes. The arch, along with the posterior aspect

of the body, form the spinal canal that contains and protects the spinal cord. The articular processes connect from superior to inferior among neighboring vertebrae and form a facet joint, which maintain alignment and allow for range of motion².

The thoracic spine has several unique features. First, is the presence of costal facets and associated ribs. Six costal facets are present on each thoracic vertebrae—1 on each transverse process and 2 demi-facets on each side of the vertebral body. These costal facets articulate with the posterior ribs at each respective level² (Figure 2). Together, and with the combination of the anterior axial skeleton, the ribcage is formed. The ribcage greatly strengthens the stability of the thoracic spine compared to the other segments, with biomechanical studies having demonstrated significant differences in range of motion in thoracic cadaveric spines with disarticulated ribs^{3,4}. Second, the natural alignment of the thoracic spine is 20-50° of kyphosis, which differs from the 20-60° of lordosis in the lumbar spine and 20-40° of lordosis in the cervical spine^{5,6}. Third, the motion of a spinal segment is determined in part by the plane of facet joint orientation⁷. In the thoracic spine, facet joints are aligned more coronally. This allows for more rotation but minimizes extension. Conversely, the more sagittal orientation of the lumbar facets allows for more extension while limiting rotation⁸ (Figure 3).

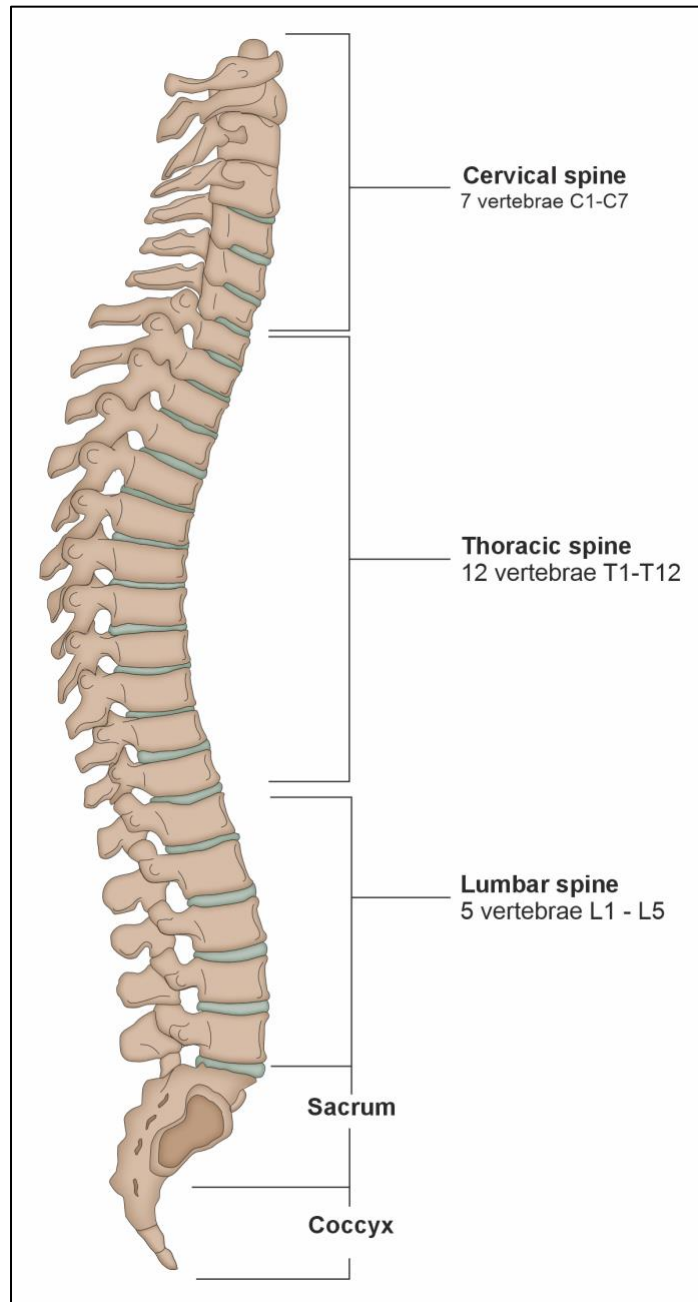


Figure 1. Anatomy of the vertebral column

The cervical and lumbar spine natural position is in lordosis, while the thoracic spine sits in kyphosis.

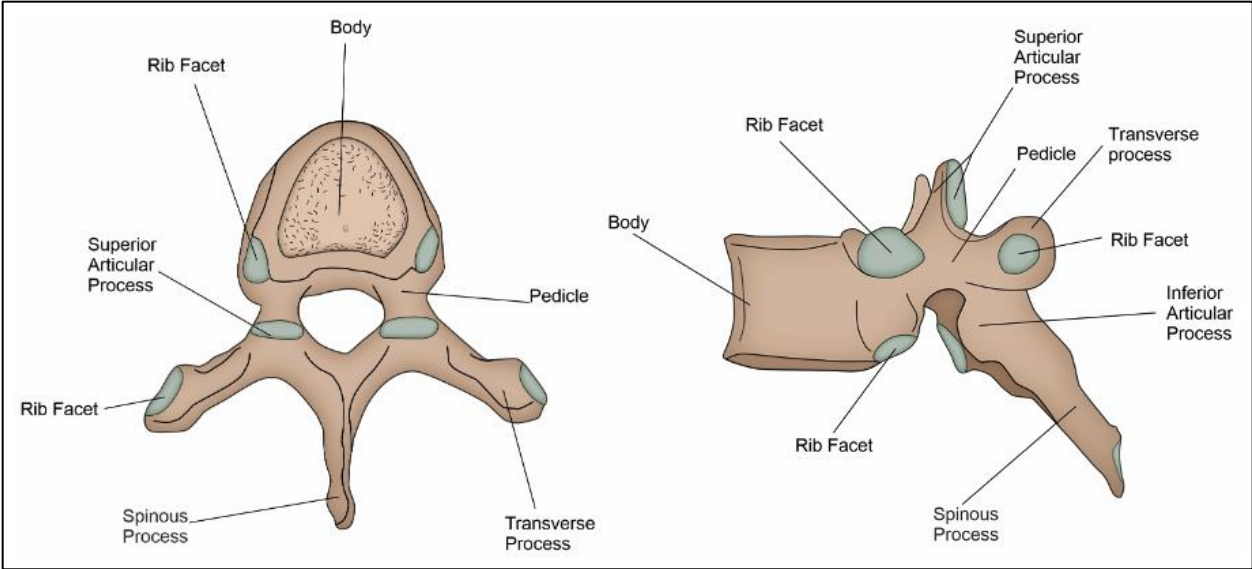


Figure 2. Anatomy of the thoracic vertebra

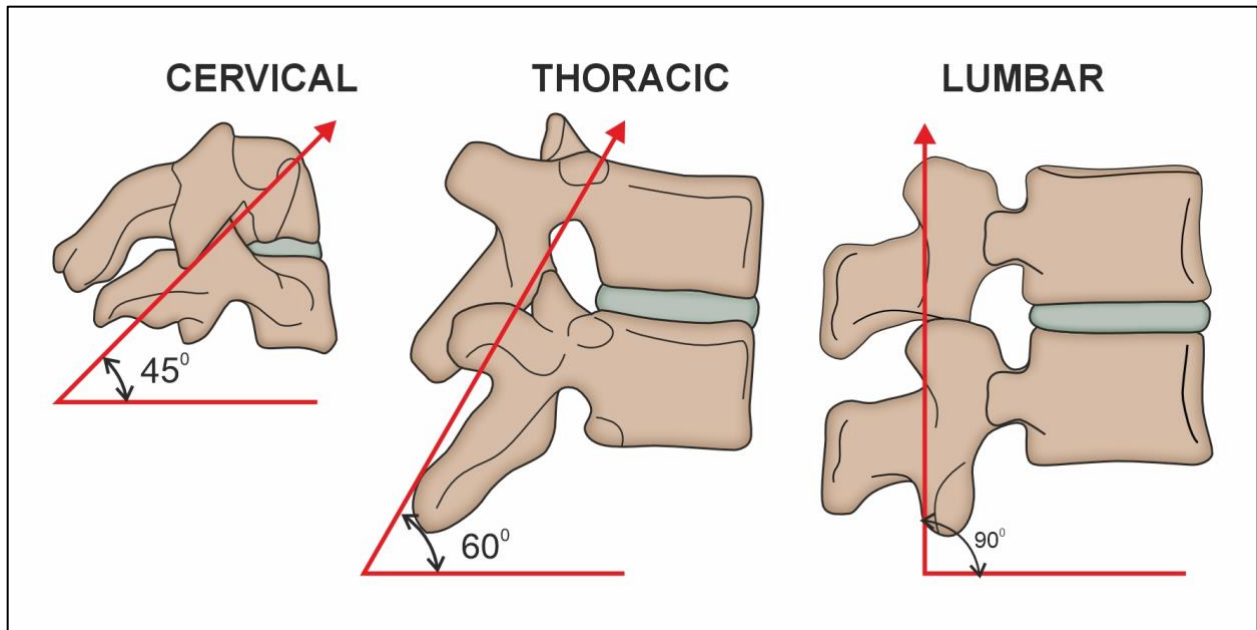


Figure 3. Apophyseal Joint orientation variation

Anatomical differences of the facet joints in cervical, thoracic, and lumbar vertebrae. Cervical facet joint orientation is more transverse, while thoracic is more coronal and lumbar is more sagittal⁷.

1.2 – PSEUDARTHROSIS AND IMPLANT-RELATED COMPLICATIONS

Spinal fusion surgery continues to be a mainstay in the treatment of traumatic and degenerative conditions. One population-based study, comparing rates of fusion procedures from 2004 to 2015, showed a 32% increase in the number of surgeries in that timeframe⁹. Unfortunately, these fusion surgeries are not always successful, and with the increase in incidence of spinal fusion surgeries, there is also an increase in the incidence of revision spine surgeries. There are multiple reasons why patients may require revision surgery, but the remainder of this work will focus on pseudarthrosis and its relation to implant-related complications.

Pseudarthrosis, or nonunion, is a failure of fusion diagnosed at or after 1 year of index surgery¹⁰. In a population based review of revision surgery following lumbar spine surgery, 23.6% of revision surgeries were done for pseudarthrosis¹¹. Although, spinal implants can fail in multiple ways—such as screw malposition or fracture, rod dislodgement, interbody cage subsidence, or painful or prominent implants^{12,13}—rod fracture accounts for approximately 47-60% of the total^{1,14} and is one of the most common implant-related complications. Rod fracture is closely linked to pseudarthrosis, where the odds of having a rod fracture in the setting of pseudarthrosis is 29 times greater than having a rod fracture without pseudarthrosis¹⁵.

The link between pseudarthrosis and rod fracture is a double-edged sword. If rod fracture occurs early after surgery (typically within 1 year), it is thought to be due to increased mobility across the fusion site, causing increased strain on the rod, which leads to fracture. This then causes further increased mobility at the fusion site leading to pseudarthrosis¹⁵. If rod fracture occurs later after surgery (usually greater than 1 year), it is thought to be due to increased mobility at the

fusion leading to an inability of the segments to fuse. This then results in increased cyclical loading of the rod construct, increased micro-movements, increased construct strain, and ultimately, instrumentation failure¹⁶⁻¹⁹. In both these settings, increasing construct stiffness is thought to be a way to decrease the prevalence of pseudarthrosis and rod fracture²⁰.

1.3 – INCREASING ROD STIFFNESS

Spinal construct stiffness can be increased by performing an interbody fusion, up-sizing pedicle screw instrumentation, or by augmenting the posterolateral fusion mass with increased rod stiffness²¹. For the purposes of this topic, we will focus solely on methods to increase rod stiffness, which can be accomplished by changing the material or shape, increasing the diameter, or increasing the number of rods^{22,23}.

1.3.1 – ROD MATERIAL

Commonly used metal rods in spine surgery include titanium alloy, stainless steel, and cobalt chromium alloy. Out of these three materials, titanium appears to afford the least amount of stiffness. In one study looking at twenty-four implants that were mounted in polyethylene blocks and subsequently cyclically loaded, stainless steel implants demonstrated greater stiffness than titanium alloy implants²⁴. Additionally, in a 1997 biomechanical analysis comparing titanium to stainless steel embedded in ultra-high molecular weight polyethylene blocks, the stiffness of stainless steel constructs was significantly higher than titanium ones²⁵. Similarly, in a 2018 study, titanium was shown to afford less stability than cobalt chromium²⁶.

Whether stainless steel or cobalt chromium provides more stability is less clear though. In a 2009 biomechanical study, researchers compared titanium to cobalt chromium in a 4-point bending mechanical testing with the goal of understanding how these rods of different material differ with regards to bending stiffness, strength (as expressed by yield point), and memory (deformation at yield point). Cobalt chromium demonstrated similar Young's Modulus to high-strength steel, but greater Young's Modulus than standard-strength steel²⁷. On the other hand, in a retrospective

review, cobalt chromium and stainless steel were compared in patients undergoing spinal deformity surgery. The incidence of rod fracture in those with cobalt chromium rods was 15% compared to 8% in those with stainless steel rods²⁸. Together, these studies suggest high amount of stiffness in both stainless steel and cobalt chromium, with perhaps more overall stiffness in cobalt chromium and more variability in stiffness within stainless steel ones.

1.3.2 – ROD DIAMETER

Increasing rod diameter is another way to increase overall construct stiffness. This has been shown in both biomechanical and clinical studies. In a 2007 biomechanical in vitro analysis on bovine spines undergoing physiologic loading after anterior scoliosis instrumentation, researchers compared the stress seen across different sized stainless steel rods. They demonstrated increased stiffness in 5mm rods compared to 4mm rods²⁹. Later, in 2011, a separate group conducted a biomechanical analysis on the cervicothoracic junction in cadaveric spines with ankylosing spondylitis. Their results demonstrated greater stiffness in 3.5mm titanium rods compared to 3.2mm titanium rods³⁰.

1.3.3 – ROD SHAPE

Potentially less studied than rod material and diameter, is the concept of rod shape. In a 2002 geometric element model and analysis, researchers compared rods with a cross-sectional square shape and those with a cross-sectional circular shape. Overall, they demonstrated better biomechanical performance in square-shaped rods³¹. To the best of our knowledge, no further studies have followed up on or demonstrated these findings clinically, potentially due to

manufacturers of these implants not having widely fabricated this design, thus limiting their clinical relevance.

1.3.4 – NUMBER OF RODS

Among the methods to increase rod stiffness, the most researched method is using additional metal rods to create a multiple-rod construct (MRC) instead of the standard 2-rod or dual-rod construct (DRC). Essentially, an MRC can be made by attaching additional rods alongside the existing left and right posterior rods, for a total of 3 or more rods. Indeed, multiple studies have shown success in reducing the number of rod fractures with MRCs compared to DRCs^{14,32–35}.

One retrospective review from 2019 examined 106 patients with adult spinal deformity and compared those with MRCs to those with DRCs with the goal of determining the incidence of iliac screw loosening. Patients with MRCs had a higher incidence of iliac screw loosening but lower rate of rod fractures compared to those with a DRCs³².

In 2021, accessory rod constructs were compared to traditional DRCs in a cohort of patients with adult spinal deformity. The results from this study showed a decreased incidence of rod fractures in the accessory rod (i.e. MRC) group, despite that group having higher baseline deformity and a higher rate of pedicle subtraction osteotomy³³.

On the other hand, in 2021, Bourghli et al. published a retrospective review of 67 patients with adult spinal deformity who underwent pedicle subtraction osteotomy and were fused with an MRC or standard DRC. They showed similar rates of rod-related complications between the two

cohorts, as well as similarities between complications associated with pseudarthrosis. However, in this cohort, better patient-reported outcome scores and postoperative coronal alignment were observed in the MRC group compared to the DRC group³⁶.

1.4 – THESIS RATIONALE

Much of the biomechanical work supporting the use of MRCs to increase stiffness has been conducted on cadaveric lumbar spines, or biomechanical models of the lumbar spine^{37,38}.

Largely, this research has focused on increasing stiffness in the setting of concurrent osteotomy for adult spinal deformity³⁹⁻⁴³.

Although the biomechanical investigation into adult spinal deformity and the various osteotomies that are done to treat such pathology in the lumbar spine are well deserved, the use of MRCs in the thoracic spine is still an area not as well researched. Rod fractures can certainly occur in the thoracic spine as well, such as in tumor resection surgery⁴⁴, where the thoracic spine is the most common region for cancer metastasis⁴⁵. Additionally, in adult patients operated on for scoliosis without osteotomies, where long constructs can span the length of the thoracic and lumbar spine, rod fractures have been reported at a rate of 4%⁴⁶.

To the best of our knowledge, no biomechanical analysis of MRCs has been conducted in the thoracic spine. The purpose of this thesis is to compare the stability of MRCs to DRCs in cadaveric thoracic spines. Our hypothesis is that MRCs will demonstrate increased stability compared to DRCs. A secondary objective of this thesis is to examine the behavior of screw loosening and segmental changes in these two constructs after a 1-hour fatigue test.

CHAPTER 2

2 – METHODS

This chapter gives an overview around the various materials and methodology used in this thesis.

2.1 – CADAVER PREPARATION

Prior to specimen collection and preparation, approval was obtained from the institutional ethics board (ID#118078 and ID#125155). Full details around the initial collection and preparation of these specimens is detailed elsewhere⁴⁷. Briefly, 11 full cadaveric specimens were procured and included non-identifiable information such as medical history, cause of death, age, and sex. All specimens were kept in -20°C freezer prior to use. Computed tomography (CT) scan was then performed to rule out internal bony abnormalities.

Once the CT scan was complete, specimens were sectioned into cervical, thoracic, and lumbosacral segments. The thoracic spine (T1-T12) segment was used for this study. These specimens were then thawed to room temperature and prepared further. The majority of musculature was dissected off the specimen, leaving the facet capsules, posterior ligamentous complex, and costovertebral joints intact. The ribcage was removed leaving approximately 2cm of posterior rib attached at the costovertebral joints. The most cranial (T1) and most caudal (T12) vertebral segments were then potted in cement with their endplates parallel to the ground, leaving the adjacent intervertebral discs free and able to allow range of motion. This setup can be seen in Figure 4. From here, all spines underwent native range of motion testing without

instrumentation and were subsequently instrumented for non-destructive testing as part of a previous study⁴⁷. Following this testing, all spines were stored back in a freezer at -20°C.

After reviewing the specimens' imaging and medical history, preliminary testing of cadaveric spines for the present study was then conducted to develop the testing protocol. During this preliminary testing, 2 of the initial 11 cadaveric specimens sustained bony or ligamentous damage and were subsequently excluded from the present study. As such, 9 thoracic spines were non-damaged and available for further biomechanical testing. Demographics of cadaveric specimens used in this study are detailed in Table 1.

Table 1. Demographics of cadaveric specimens.

Specimen	Age	Sex	Cause of Death
1	62	Male	Respiratory Failure
2	68	Male	Respiratory Failure
3	65	Male	Cholangiocarcinoma
4	72	Female	Paget's Disease
5	71	Male	Cardiac Arrest
6	33	Male	Head Injury
7	78	Male	Lymphoma
8	63	Female	Respiratory Failure
9	69	Male	Cardiomyopathy



Figure 4. Cadaveric Specimen Preparation

Cadaveric thoracic spines (T1-T12) were sectioned and cleared of any musculature. They were then potted into cement at the cranial (T1) and caudal (T12) ends. The T1-T2 and T11-T12 articulation are free to allow motion.

2.2 – INSTRUMENTATION

Prior to instrumentation and testing, specimens were thawed overnight at room temperature. Multi-level pedicle screw fixation was performed starting from T3 and extending down to include T11—this left T2 as an uninstrumented level, while T1 and T12 were both fixed in potted cement. Pedicle screw start point and insertion technique was done according to previously described technique⁴⁸. Using a pedicle probe, screw tracts were examined for breaches. The depth of each screw track was then measured, and 6.0mm polyaxial pedicle screws were inserted, ranging from 40mm to 55mm in length. Pedicle screws were inserted by hand to ensure a constant angle and speed until each screw was well seated.

From here, specimens were randomized to undergo either initial testing with a multiple-rod construct (MRC) or with a dual-rod construct (DRC). To create a DRC, one 5.5mm diameter titanium rod was bent to the appropriate shape and attached to the left-sided pedicle screws spanning from T3-T11, while a second rod was attached to the right-sided pedicle screws. Both rods were then secured in place to the pedicle screws with locking set screws. To create an MRC, the same process was done that was used for the DRC set-up, followed by placement of one additional 5.5mm titanium rod just lateral to the existing 2 rods, with each new rod secured in place with one 5.5mm-5.5mm rod-to-rod connector cranially between T3 and T4 pedicle screws, and one 5.5mm-5.5mm rod-to-rod connector caudally between T10 and T11 pedicle screws. This resulted in a total of 4 rods in the MRC set-up. An example of the DRC and MRC setups can be seen in Figure 5.

After completing instrumentation, markers were rigidly applied to the specimens to create landmarks to be captured with the digital imaging correlation system. These markers included twelve 2.0mm K-wires with attached 3D-printed hemispherical plastic components covered with multiple black and white contrasting stickers. One of these markers was inserted into each vertebral body spanning from T1-T12. An example of this construct and marker setup is seen in Figure 6.

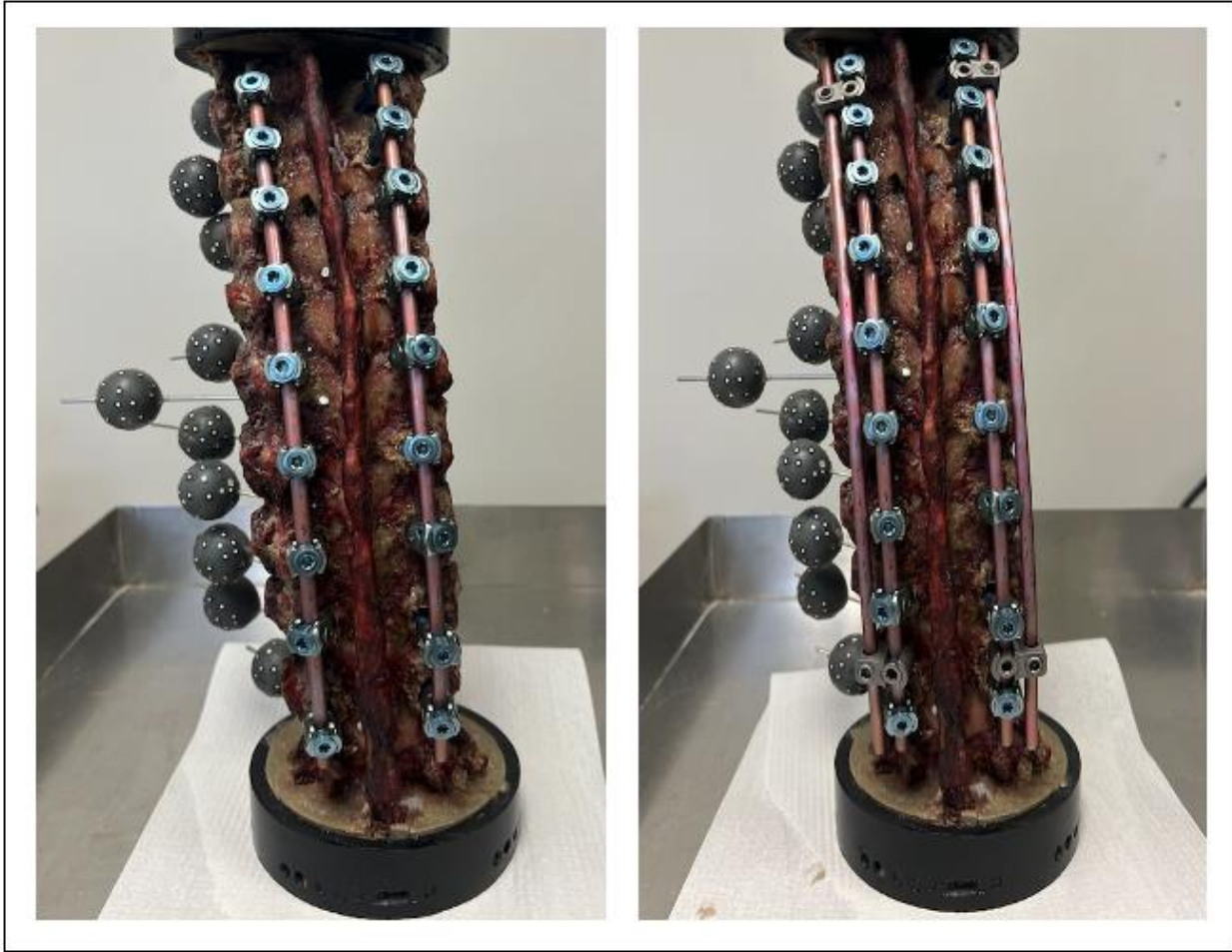


Figure 5. Instrumentation of dual-rod and multiple-rod constructs

Cadaveric thoracic specimens were instrumented from T3 to T11. Rods were applied bilaterally and fixed into place with locking set screws to create a dual-rod construct (left). To create the multiple-rod construct, an additional rod was placed bilaterally spanning the fusion site and held in place by 2 rod-to-rod connectors, one between T3-T4 and one between T10-T11 (right).



Figure 6. Attachment of markers for digital image correlation system

Twelve 2.0mm K-wires with attached 3D-printed hemispherical plastic components were covered with pre-calibrated black and white stickers to allow tracking from the digital imaging correlation system. One of these markers was inserted into each vertebral body spanning from T1-T12.

2.3 – SPECIMEN TESTING

Upon completion of instrumentation and application of markers to allow proper image capture, the potted specimens were ready for testing. Each specimen was tested individually, on separate days, one at a time. Potted specimens were mounted on a testing machine with custom design modifications (Instron® 5967, Norwood, MA, USA). The potted T12 was rigidly attached to a sliding x-y table allowing unrestricted translation motion in the transverse plane. The potted T1 was rigidly attached to a custom testing jig capable of testing in six degrees of freedom. An example of this set up is seen in Figure 7.

First, range of motion (ROM) tests were performed with the intact spines prior to fusion. Then ROM tests were done following initial instrumentation (either DRC or MRC). The specimens were preloaded with 15N of force and set to maintain 15N during the test to remove any mechanical slack and aid in mounting the specimen through its neutral axis. ROM testing involved applying a pure rotational or bending load to the most cranial (T1) end up to a limit of $\pm 5\text{Nm}$, at 1° per second, and cycled three times with the first two cycles for preconditioning and the last for data analysis. This method was based on previous protocols⁴⁹.

ARAMIS Adjustable 12M system (GOM Metrology, Braunschweig, Germany) was used as a digital imaging correlation (DIC) system to track the motion in six degrees of freedom of the twelve previously inserted 3D printed markers rigidly attached to each vertebra. The setup consisted of two 24mm focal length and 4096-by-3600 pixels (pixel size of $3.45\mu\text{m}$) resolution cameras. The two cameras were set at a 25° angle, 4 Hz, and illuminated with two polarized LED light sources. The DIC setup was calibrated prior to each biomechanical test by a standard calibration protocol and calibration plate provided by GOM Metrology for a measuring volume

of 570-by-430-by-430mm. The images were processed in ARAMIS Professional 2019 (GOM Metrology, Braunschweig, Germany). Torsion was applied and tracked by a universal testing device (Instron® 5967, Norwood, MA, USA) using a 50kN load cell recording data at 50Hz. Load cells were able to measure both forces as well as moments. Bending was applied and tracked by a custom testing jig consisting of a stepper motor (NEMA 23, OMC) and a 2.2kN load cell (MC3A-6-1k, AMTI) recording data at 20Hz. Each specimen was tested in flexion/extension, lateral bending, and internal/external rotation in a random order.

Next, the specimens were cyclically loaded during a 1-hour extended test to simulate a scenario of day-to-day wear and tear of the construct before bony fusion. Again, the spines were preloaded to 15N to remove mechanical slack and to aid in mounting through the neutral axis. The specimens were tested for one hour and were cyclically loaded in IR/ER to $\pm 5\text{Nm}$ at 5° per second and a cyclically applied axial load from 200N to 350N (representing one-quarter and one-half body weight respectively) at 150N/s for one hour. Cyclical axial loads and cyclic torsional loads were independently applied. The torque data was captured by the same load cell as above (30kN load cell at 50Hz), while the positional/rotational data was collected in a predefined pulsed setup by the DIC system. The pulsed sequence was set to record the first 20 seconds at 10Hz, then to reduce file size, this was set to record data at 1/3Hz for the next 3560 seconds before recapturing the data at 10Hz for the last 20 seconds of the one-hour test. The DIC system recorded the position of the 12 vertebrae throughout time.

Immediately following the extended duration test, specimens were examined for any evidence of bony or ligamentous failure. Additionally, all screw-bone interfaces and screw-rod interfaces

were examined for signs of loosening. After thorough inspection, if no damage was visualized, the specimens were tested once again in flexion/extension, lateral bend, and rotation. This was done in an effort to determine if any change in motion was observed following the extended duration test. The testing sequence of ROM to extended test to ROM was then repeated for the other construct with the same specimen.

ROM was calculated as the difference between the maximum and minimum ROM at each vertebra.

$$ROM_x = ROM_{x,max} - ROM_{x,min}$$

Where, the subscript *max* and *min* are the maximum and minimum recorded values, respectively, and ROM_x is the range of motion at the targeted vertebra.

The stiffness of the vertebra was calculated by taking the slope of the entire torque rotation curve:

$$Stiffness = \frac{(moment_{max} - moment_{min})}{(ROM_{max} - ROM_{min})}$$

Where $moment_{max}$ is the maximum moment recorded (i.e., 5Nm), $moment_{min}$ is the minimum moment recorded (i.e., -5Nm), ROM_{Max} is the maximum rotation/bending recorded for T1, and ROM_{min} is the minimum rotation/bending recorded for T1.

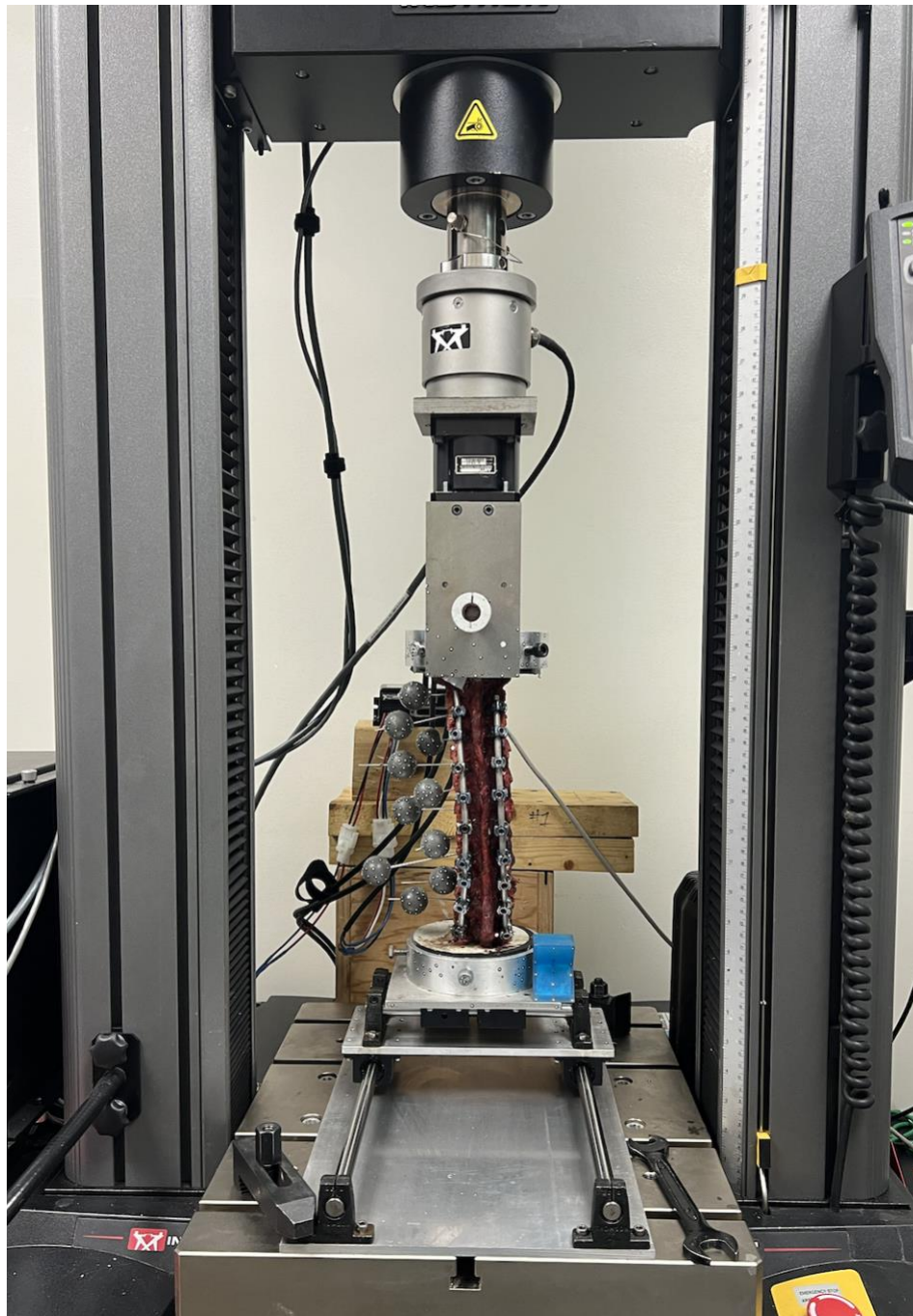


Figure 7. Biomechanical testing set-up

The potted and instrumented spines were mounted onto a custom table-top testing machine and secured at the top and bottom. Various loads were applied in each plane of motion and the optical tracking system monitored motion at the different segments.

2.4 – STATISTICAL ANALYSIS

SPSS statistical software (version 29) was used for the statistical analysis of captured data. Each cadaveric specimen acted as its own control. Wilcoxon signed-rank test was used to compare median differences in total range of motion and total stiffness between construct types (i.e. DRC vs. MRC) and between status of fatigue test (i.e. pre- vs. post-). Statistical significance was set at <0.05 . Additionally, individual segment range of motion median differences were compared using the Wilcoxon signed-rank test with statistical significance set at <0.05 . T1-T2 and T11-T12 were excluded from the analysis as the T1 and T12 vertebral bodies were fixed in cement.

CHAPTER 3

3 – RESULTS

This chapter details the results of the biomechanical testing. In total, 9 specimens were tested after being instrumented with a dual-rod or multiple-rod construct. All tests were completed successfully. No qualitative defects in bone, ligament, or hardware were observed throughout any of the testing.

3.1 – TOTAL RANGE OF MOTION AND STIFFNESS

When comparing the two construct types before and after the 1-hour bodyweight simulation test, range of motion (ROM) was higher for rotation, lateral bend, and flexion/extension for DRCs post-fatigue testing. For MRCs, rotation and lateral bend ROM were significantly higher after testing, while flexion/extension was not significantly different. Similarly, stiffness was lower following the 1-hour test for rotation and lateral bend in both DRCs and MRCs. However, flexion/extension was lower post-fatigue testing for DRC, but not for MRC (Table 2). No significant differences in absolute ROM or stiffness were found between DRCs and MRCs, regardless of the status of fatigue test or plane of motion (Table 3). A graphical comparison of construct ROM is shown in Figure 8.

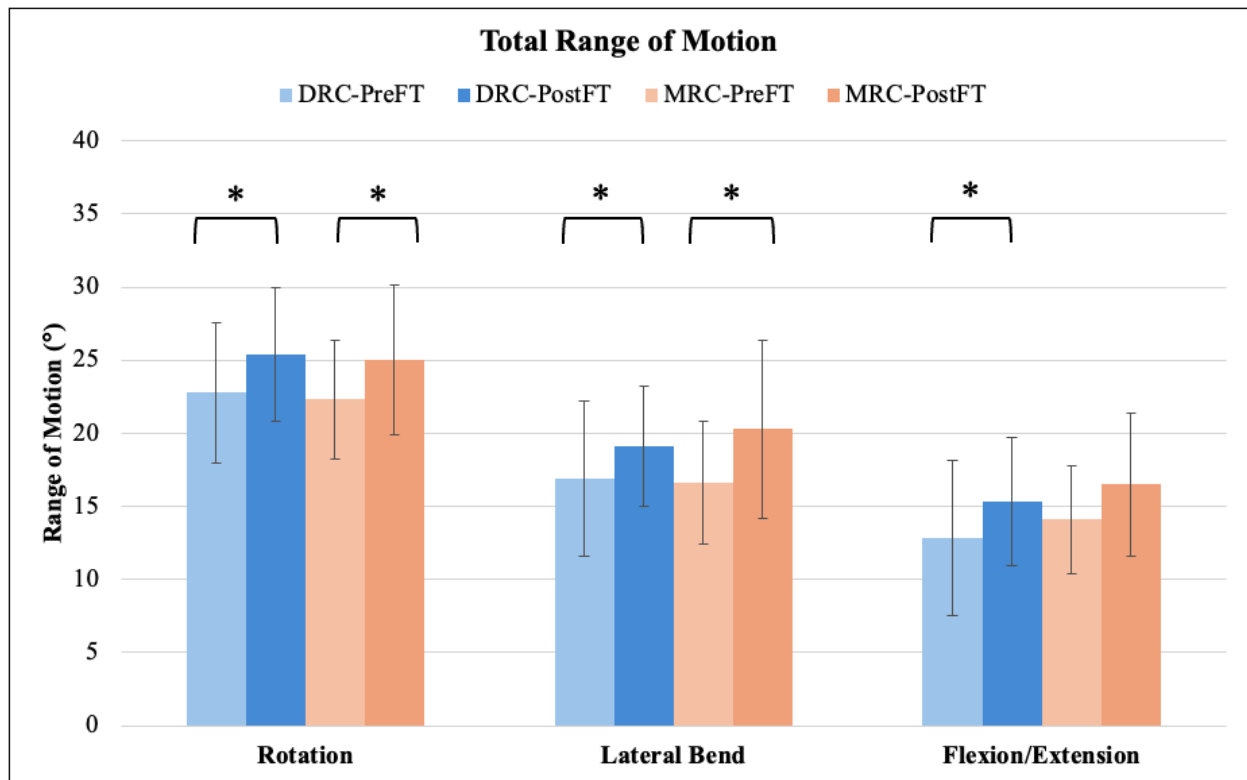


Figure 8. Graphical comparison of total range of motion

No significant differences in range of motion, regardless of fatigue status and plane of motion, were observed between multiple-rod and dual-rod constructs. In all planes of motion, however, range of motion was higher after 1-hour fatigue testing for both construct types, except for flexion/extension, which was similar for multiple-rod constructs before and after 1 hour fatigue testing.

Abbreviations: DRC = dual-rod construct, MRC = multiple-rod construct, PreFT = test performed prior to 1-hour simulated fatigue test, PostFT = test performed after 1-hour simulated fatigue test.

3.1.1 – ROTATION

Mean ROM was significantly higher after 1-hour testing for DRC ($25.4 \pm 4.6^\circ$ vs. $22.8 \pm 4.8^\circ$, $p = 0.009$) and for MRC ($25.0 \pm 5.1^\circ$ vs. $22.3 \pm 4.1^\circ$, $p = 0.009$). Stiffness was significantly lower after 1-hour testing for DRC ($0.41 \pm 0.08\text{Nm}^\circ$ vs. $0.46 \pm 0.09\text{Nm}^\circ$, $p = 0.009$) and for MRC ($0.42 \pm 0.09\text{Nm}^\circ$ vs. $0.47 \pm 0.09\text{Nm}^\circ$, $p = 0.009$). ROM and stiffness were similar between DRC and MRC regardless of fatigue status.

3.1.2 – LATERAL BEND

Mean lateral bend ROM was significantly higher after 1-hour testing for DRC ($19.1 \pm 4.1^\circ$ vs. $16.9 \pm 5.3^\circ$, $p = 0.009$) and for MRC ($20.3 \pm 6.1^\circ$ vs. $16.6 \pm 4.2^\circ$, $p = 0.009$). Stiffness was significantly lower after 1-hour testing for DRC ($0.58 \pm 0.13\text{Nm}^\circ$ vs. $0.67 \pm 0.17\text{Nm}^\circ$, $p = 0.009$) and for MRC ($0.56 \pm 0.16\text{Nm}^\circ$ vs. $0.66 \pm 0.17\text{Nm}^\circ$, $p = 0.009$). ROM and stiffness were similar between DRC and MRC regardless of fatigue status.

3.1.3 – FLEXION/EXTENSION

Mean flexion/extension ROM was significantly higher after 1-hour testing for DRC ($15.3 \pm 4.4^\circ$ vs. $12.8 \pm 5.3^\circ$, $p = 0.009$) but not for MRC ($16.5 \pm 4.9^\circ$ vs. $14.1 \pm 3.7^\circ$, $p = 0.076$). Stiffness was significantly lower after 1-hour testing for DRC ($0.76 \pm 0.31\text{Nm}^\circ$ vs. $1.13 \pm 1.08\text{Nm}^\circ$, $p = 0.009$). Stiffness was also lower for MRC after 1-hour testing but did not reach statistical significance ($0.70 \pm 0.22\text{Nm}^\circ$ vs. $0.80 \pm 0.23\text{Nm}^\circ$, $p = 0.058$). ROM and stiffness were similar between DRC and MRC regardless of fatigue status.

Table 2. Total Range of Motion and Stiffness, comparison by fatigue status

Test Scenario	Total ROM (°)		P-Value	Total Stiffness (Nm/°)		P-Value
	Mean (SD)			Mean (SD)		
	Pre-FT	Post-FT		Pre-FT	Post-FT	
Dual-Rod Construct						
Rotation	22.8 (4.8)	25.4 (4.6)	0.009	0.46 (0.09)	0.41 (0.08)	0.009
Lateral Bend	16.9 (5.3)	19.1 (4.1)	0.009	0.67 (0.17)	0.58 (0.13)	0.009
Flexion/Extension	12.8 (5.3)	15.3 (4.4)	0.009	1.13 (1.08)	0.76 (0.31)	0.009
Multiple-Rod Construct						
Rotation	22.3 (4.1)	25.0 (5.1)	0.009	0.47 (0.09)	0.42 (0.09)	0.009
Lateral Bend	16.6 (4.2)	20.3 (6.1)	0.009	0.66 (0.17)	0.56 (0.16)	0.009
Flexion/Extension	14.1 (3.7)	16.5 (4.9)	0.076	0.80 (0.23)	0.70 (0.22)	0.058

Abbreviations: ROM = range of motion, Pre-FT = test performed prior to 1-hour simulated fatigue test, Post-FT = test performed after 1-hour simulated fatigue test.

P-values obtained from two-sided Wilcoxon test. Bolded values are <0.05.

Table 3. Total Range of Motion and Stiffness, comparison by construct

Test Scenario	Total ROM (°)		P-Value	Total Stiffness (Nm/°)		P-Value
	Mean (SD)			Mean (SD)		
	DRC	MRC		DRC	MRC	
Pre-Fatigue Test						
Rotation	22.8 (4.8)	22.3 (4.1)	0.722	0.46 (0.09)	0.47 (0.09)	0.813
Lateral Bend	16.9 (5.3)	16.6 (4.2)	0.477	0.67 (0.17)	0.66 (0.17)	0.554
Flexion/Extension	12.8 (5.3)	14.1 (3.7)	0.076	1.13 (1.08)	0.80 (0.23)	0.124
Post-Fatigue Test						
Rotation	25.4 (4.6)	25.0 (5.1)	0.343	0.41 (0.08)	0.42 (0.09)	0.236
Lateral Bend	19.1 (4.1)	20.3 (6.1)	0.554	0.58 (0.13)	0.56 (0.16)	0.554
Flexion/Extension	15.3 (4.4)	16.5 (4.9)	0.286	0.76 (0.31)	0.70 (0.22)	0.554

Abbreviations: DRC = dual-rod construct, MRC = multiple-rod construct, ROM = range of motion.

P-values obtained from two-sided Wilcoxon test. Bolded values are <0.05.

3.2 – RANGE OF MOTION BY VERTEBRAL SEGMENT

Overall, the range of motion at the first uninstrumented level (T2-T3) was significantly higher in all planes of motion after 1-hour fatigue testing than before, but there were no differences between DRC or MRC. As testing moved caudally, these differences were less pronounced. A detailed analysis of ROM for all measured vertebral levels is found in Table 4. All range of motion was $<1^\circ$ at T5-T6 and distal, and there were no significant differences in motion between construct type or status of fatigue testing. As such, ROM values for T5-T6 were omitted from Table 4.

Table 4. Range of Motion by Vertebral Segment

Vertebral Level	Direction of Motion	Fatigue Test Pre vs. Post	Dual Rod-Construct		Multiple-Rod Construct		P-Value
			ROM (°) Mean (SD)	P-Value Pre vs. Post	ROM (°) Mean (SD)	P-Value Pre vs. Post	DRC vs. MRC
T2-T3	Rotation	Pre	7.37 (2.60)	0.009	7.75 (2.47)	0.033	0.554
		Post	8.61 (2.54)		8.73 (2.89)		0.906
	Lateral Bend	Pre	6.19 (2.44)	0.018	6.30 (2.46)	0.009	0.813
		Post	7.34 (2.81)		8.04 (2.69)		0.236
	Flexion/Extension	Pre	4.25 (2.36)	0.015	4.48 (2.07)	0.028	0.314
		Post	4.91 (2.21)		4.87 (1.90)		0.515
T3-T4	Rotation	Pre	1.39 (0.71)	0.018	1.28 (0.70)	0.013	0.906
		Post	1.82 (1.08)		1.80 (0.95)		1.000
	Lateral Bend	Pre	0.89 (0.59)	0.042	1.00 (0.91)	0.343	0.477
		Post	1.20 (0.81)		1.18 (1.41)		0.234
	Flexion/Extension	Pre	0.38 (0.36)	0.024	0.59 (0.47)	0.076	0.554
		Post	0.74 (0.70)		0.94 (1.06)		0.636
T4-T5	Rotation	Pre	0.67 (0.28)	0.343	0.64 (0.28)	0.044	0.813
		Post	0.76 (0.38)		0.75 (0.38)		0.906
	Lateral Bend	Pre	0.10 (0.11)	0.624	0.07 (0.09)	0.813	0.155
		Post	0.08 (0.12)		0.09 (0.14)		0.441
	Flexion/Extension	Pre	0.09 (0.10)	0.097	0.04 (0.09)	0.477	1.000
		Post	0.12 (0.08)		0.07 (0.14)		0.097

Abbreviations: ROM = range of motion, Pre = test performed prior to 1-hour simulated fatigue test, Post = test performed after 1-hour simulated fatigue test, DRC = dual-rod construct, MRC = multiple-rod construct.

P-values obtained from two-sided Wilcoxon test. Bolded = P-Value <0.05.

Note: T2-T3 is uninstrumented, while T3-T4 and T4-T5 are first and second instrumented levels, respectively. From T5-T11, ROM is negligible with all values <1°.

3.2.1 – ROTATION BY VERTEBRAL SEGMENT

At T2-T3, mean rotation was significantly higher post 1-hour fatigue test for DRC ($8.61 \pm 2.54^\circ$ vs. $7.37 \pm 2.60^\circ$, $p = 0.009$) and for MRC ($8.73 \pm 2.89^\circ$ vs. $7.75 \pm 2.47^\circ$, $p = 0.033$). Rotation between MRC and DRC at this level was similar regardless of fatigue test status.

At T3-T4, mean rotation was significantly higher post-1 hour fatigue test for DRC ($1.82 \pm 1.08^\circ$ vs. $1.39 \pm 0.71^\circ$, $p = 0.018$) and for MRC ($1.80 \pm 0.95^\circ$ vs. $1.28 \pm 0.70^\circ$, $p = 0.013$). Rotation between MRC and DRC at this level was similar regardless of fatigue test status.

At T4-T5, mean rotation was similar post 1-hour fatigue test for DRC ($0.76 \pm 0.38^\circ$ vs. $0.67 \pm 0.28^\circ$, $p = 0.343$) but greater for MRC ($0.75 \pm 0.38^\circ$ vs. $0.64 \pm 0.28^\circ$, $p = 0.044$). Rotation between MRC and DRC at this level was similar regardless of fatigue test status. Graphical depiction of rotation ROM by vertebral level is shown in Figure 9.

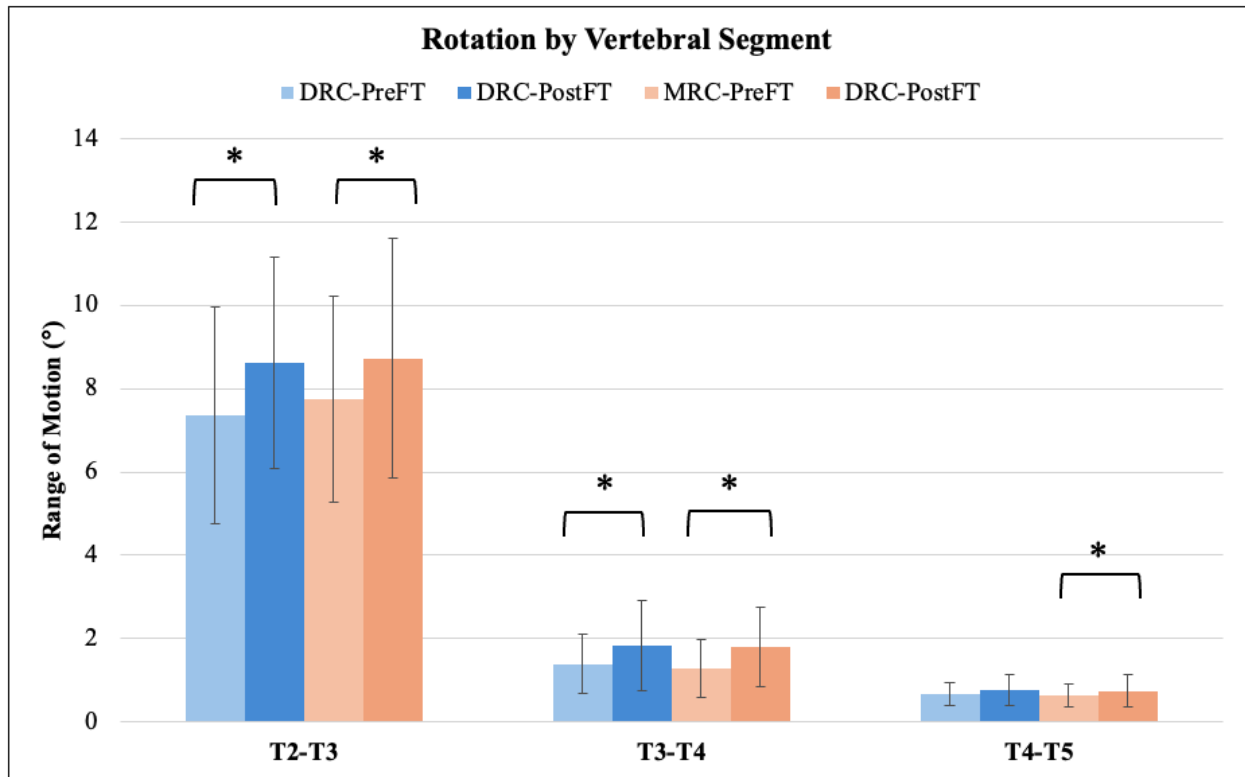


Figure 9. Rotation by vertebral segment.

No significant differences in range of motion, regardless of fatigue status, were observed between multiple-rod and dual-rod constructs. At T2-T3 and T3-T4, range of motion was higher after 1-hour fatigue testing for both construct types. At T4-T5, range of motion was higher after 1-hour fatigue testing for multiple-rod constructs only.

* Indicates Wilcoxon signed-rank test P-Value <0.05

Abbreviations: DRC = dual-rod construct, MRC = multiple-rod construct, PreFT = test performed prior to 1-hour simulated fatigue test, PostFT = test performed after 1-hour simulated fatigue test.

3.2.2 – LATERAL BEND BY VERTEBRAL SEGMENT

At T2-T3, mean lateral bend was significantly higher post 1-hour fatigue test for DRC ($7.34 \pm 2.81^\circ$ vs. $6.19 \pm 2.44^\circ$, $p = 0.018$) and for MRC ($8.04 \pm 2.69^\circ$ vs. $6.30 \pm 2.46^\circ$, $p = 0.009$).

Lateral bend between MRC and DRC at this level was similar regardless of fatigue test status.

At T3-T4, mean lateral bend was significantly higher post 1-hour fatigue test for DRC ($1.20 \pm 0.81^\circ$ vs. $0.89 \pm 0.59^\circ$, $p = 0.042$) but not for MRC ($1.18 \pm 1.41^\circ$ vs. $1.00 \pm 0.91^\circ$, $p = 0.343$).

Lateral bend between MRC and DRC at this level was similar regardless of fatigue test status.

At T4-T5, mean lateral bend was similar pre- and post-1-hour fatigue test for both DRC and MRC. No differences in ROM were observed between construct types regardless of fatigue test status. Graphical depiction of lateral bend ROM by vertebral level is shown in Figure 10.

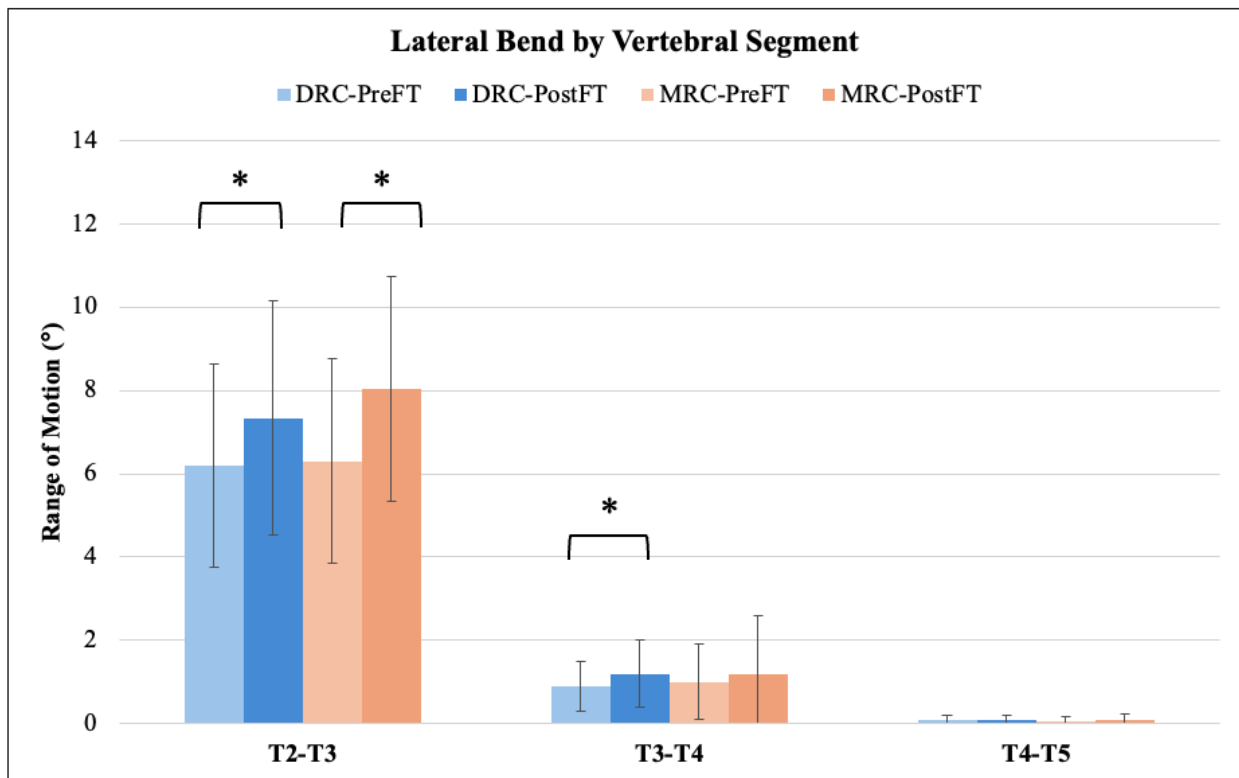


Figure 10. Lateral bend by vertebral segment.

No significant differences in range of motion, regardless of fatigue status, were observed between multiple-rod and dual-rod constructs. At T2-T3, range of motion was higher after 1-hour fatigue testing for both construct types. At T3-T4, range of motion was higher after 1-hour fatigue testing for dual-rod constructs only. No significant differences in range of motion were seen at T4-T5.

* Indicates Wilcoxon signed-rank test P-Value <0.05

Abbreviations: DRC = dual-rod construct, MRC = multiple-rod construct, PreFT = test performed prior to 1-hour simulated fatigue test, PostFT = test performed after 1-hour simulated fatigue test.

3.2.3 – FLEXION/EXTENSION BY VERTEBRAL SEGMENT

At T2-T3, mean flexion/extension was significantly higher post 1-hour fatigue test for DRC ($4.25 \pm 2.36^\circ$ vs. $4.91 \pm 2.21^\circ$, $p = 0.015$) and for MRC ($4.48 \pm 2.07^\circ$ vs. $4.87 \pm 1.90^\circ$, $p = 0.028$). No significant differences were noted in flexion/extension ROM at this level between construct type.

At T3-T4, mean flexion/extension was significantly higher post 1-hour fatigue test for DRC ($0.74 \pm 0.70^\circ$ vs. $0.38 \pm 0.36^\circ$, $p = 0.024$) but not for MRC ($0.94 \pm 1.06^\circ$ vs. $0.59 \pm 0.47^\circ$, $p = 0.076$). No significant differences were noted in flexion/extension ROM at this level between construct type.

At T4-T5, mean flexion/extension was similar between MRC and DRC regardless of construct type and status of fatigue test. Graphical depiction of flexion/extension ROM by vertebral level is shown in Figure 11.

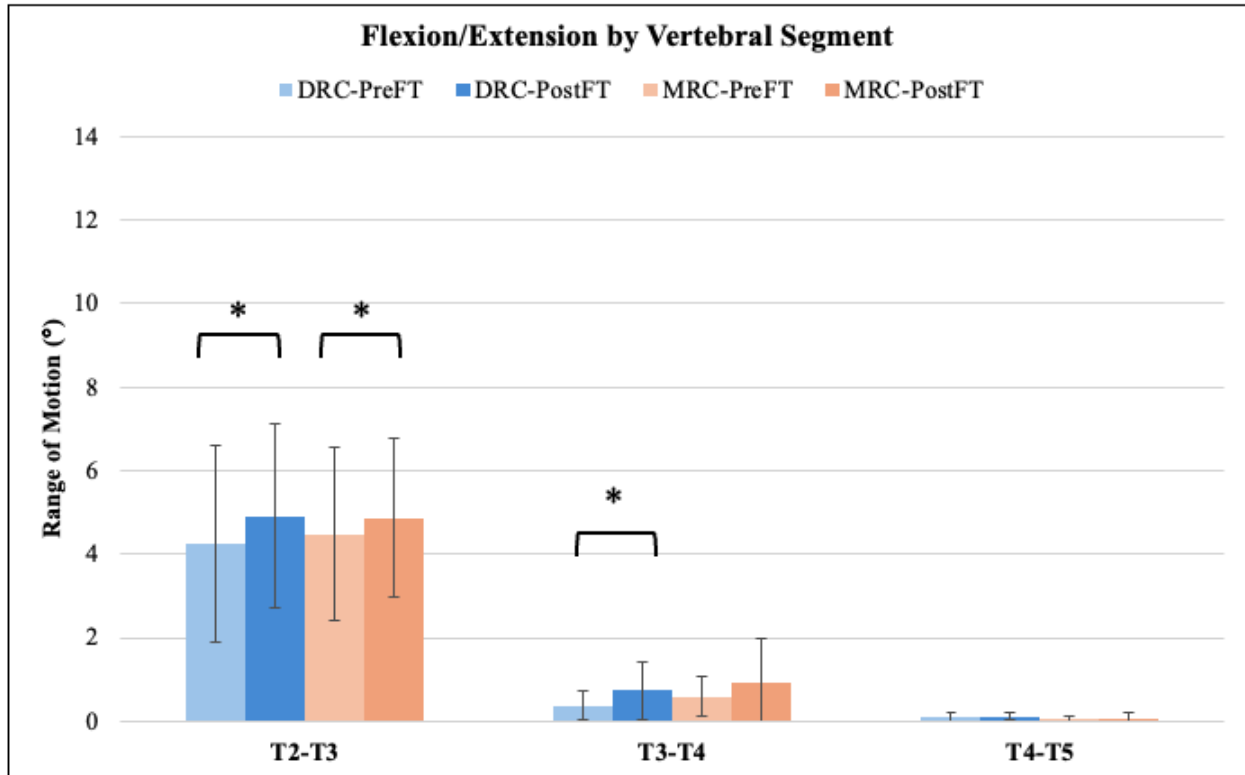


Figure 11. Flexion/Extension by vertebral segment.

No significant differences in range of motion, regardless of fatigue status, were observed between multiple-rod and dual-rod constructs. At T2-T3, range of motion was higher after 1-hour fatigue testing for both dual-rod and multiple-rod constructs. At T3-T4, range of motion was higher after 1-hour fatigue testing for dual-rod constructs only. No significant differences in range of motion were seen at T4-T5.

* Indicates Wilcoxon signed-rank test P-Value < 0.05

Abbreviations: DRC = dual-rod construct, MRC = multiple-rod construct, PreFT = test performed prior to 1-hour simulated fatigue test, PostFT = test performed after 1-hour simulated fatigue test.

CHAPTER 4

4 – DISCUSSION

This chapter includes a summary around the results of this thesis, as well as a comparison to other work performed in this field, and a look into the possible future directions for biomechanical work in this area.

4.1 – DISCUSSION AND SUMMARY

In this thesis, 9 cadaveric thoracic spines were instrumented with two different construct types—dual-rod constructs (DRC) and multiple-rod constructs (MRC). Overall range of motion and stiffness were then analyzed before and after a 1-hour bodyweight simulation fatigue test. No significant differences were observed in range of motion (ROM) or stiffness between DRCs and MRCs. However, after a 1-hour fatigue test, MRCs maintained a similar ROM and stiffness to their pre-fatigue state during flexion/extension, while DRCs did not. This suggests that MRCs may provide additional stability to daily wear and tear following initial instrumentation, thus allowing further time for a bony fusion to take place. This is supported by other biomechanical literature in the lumbar spine showing lower stress forces with MRCs^{42,43,50–52}, as well as by a recent meta-analysis comparing MRCs to DRCs in adult spinal deformity that showed lower rates of nonunion with MRCs when compared to DRCs⁵³.

An important caveat to this finding is seen, however, when the analysis is broken down into individual segments. Although DRCs and MRCs exhibited similar absolute ROM at each individual vertebral segment, they behaved differently pre- and post-fatigue testing. At the

highest instrumented level (T3-T4), only DRCs demonstrated a significantly higher ROM with lateral bend and flexion/extension post-fatigue testing. Conversely, at the T4-T5 level (second highest instrumented level), MRCs exhibited higher flexion/extension ROM while the ROM of DRCs was similar across all three movement planes pre- and post-fatigue testing. It's difficult to say what these differences translate to clinically. One hypothesis around the use of MRCs is that although they may increase overall construct stiffness and benefit fusion rates, this is achieved at the expense of increasing forces at the screw-bone interface. In a 2018 retrospective review of 106 patients with adult spinal deformity, MRCs were associated with a 1.9-fold increased risk of screw loosening at the cranial level, and a 4.1-fold increased risk of screw loosening at the caudal level³². This finding was echoed in a recent meta analysis by Zhao et al⁵³. None of the cadaveric spines tested within this thesis exhibited qualitative signs of screw-bone or screw-rod interface loosening, but it's possible that the differences in ROM at the two cranial instrumented levels post-fatigue testing were early warning signs of loosening, and with further duration of testing these differences may have become more pronounced.

Aside from nonunion, rod breakage, and screw pullout, another serious complication in long instrumented spinal surgery is proximal junctional kyphosis (PJK). PJK is defined as a sagittal Cobb angle of 10-20° between the uppermost instrumented vertebra and the vertebra 2 levels above, or when the Cobb angle between these two vertebrae is 10-15° greater than the preoperative measurement^{54,55}. This can result in new neurological deficits, fractures, severe pain, or worsening quality of life leading to revision surgery⁵⁶. The reported incidence of PJK is 5-46%⁵⁷ and its development has been linked to mechanical, tissue, and demographic risk factors, with 76% of the research focusing on mechanical contributions to PJK⁵⁵.

Among these mechanical contributions to PJK, increased rigidity of the construct at the transitional zone between instrumented and non-instrumented vertebrae is thought to play the most significant role in pathogenesis⁵⁸⁻⁶⁰, with some authors reporting lower incidence of PJK by deploying a more gradual transition in construct stiffness at the transitional level⁶¹.

Previous cadaveric work has examined semi-rigid constructs at the uppermost instrumented level and found a more linear and less abrupt change in biomechanics at the transitional zone with transverse process hooks when compared to all pedicle screws⁶². This softer transition in biomechanics is hypothesized to be protective against PJK. However, in this same analysis, semi-rigid constructs and all pedicle screw constructs were not compared to all pedicle screw constructs with multiple rods.

Although increasing construct stiffness with MRCs has been linked to increased PJK⁶³, recently, a meta-analysis explored the rates of rod fracture, pseudoarthrosis, and PJK between DRCs and MRCs. Six studies^{21,32,64-67} were included in the analysis and the meta-analysis showed no association between PJK and type of construct (DRC vs MRC)⁶⁸. In the present study, no difference in absolute range of motion was noted between DRCs and MRCs at the first uninstrumented or uppermost instrumented vertebral levels. This similarity in absolute construct stability supports the findings of this meta-analysis. However, DRCs showed increased ROM at the first instrument level (T3-T4) following 1-hour fatigue testing while MRCs did not, and at the second highest instrument level (T4-T5), MRCs showed increased ROM following 1-hour fatigue testing while DRCs did not (although the absolute ROM recorded was $<1^\circ$). This suggests that although these constructs may have initial overall comparable stiffness, they may

behave and react differently to daily wear-and-tear immediately after initial instrumentation which could ultimately affect rates of PJK. Although the clinical literature seems to indicate otherwise⁶⁹, longer duration fatigue testing is necessary to further explore this problem.

4.2 – LIMITATIONS

There were certain limitations to consider when drawing conclusions from the present analysis. The first is with the type of metal used in this experiment. Titanium rods were used in both constructs. While titanium is often the rod of choice in spine surgery, cobalt chromium is frequently used as well. It's possible that a cobalt chromium DRC and MRC may behave differently than what was observed here. Indeed, cobalt chromium constructs have been demonstrated to be more rigid than titanium ones^{26,30}, but the differences between MRC rigidity when it comes to the two materials may be overstated, as rates of PJK are not different between the two materials when MRCs are utilized⁶⁹.

Another limitation to this work is within the nature of the fatigue test that was performed. In one biomechanical study using polyethylene blocks comparing DRCs to MRCs, with 200N axial load cycled at 5Hz in the sagittal bending plane, the median number of cycles to rod failure was 59,294 in DRC, and 561,214 with MRCs⁴¹. In the present analysis, due to insufficient machine capabilities, cadaveric specimen availability, and personnel constraints, the fatigue test time had to be capped at 1-hour in order to complete specimen testing within a day. As such, the maximum number of cycles achieved during one of those time periods was never more than 1000 cycles. It's possible that with increased time and cycles, there may have been divergence in stability between the two construct types. Future endeavors should look to test the cadavers at higher cycling speeds and for longer duration of time to better ascertain the effect of prolonged stress on constructs.

Lastly, the quality of the cadaveric soft tissues should be considered within this biomechanical analysis. In this study, paraspinal musculature and ribcages were dissected off of specimens to facilitate instrumentation and testing, but this state likely does not adequately reflect in-vivo conditions as these structures play a significant role in overall thoracic spine stability^{4,70}.

4.3 – CONCLUSION

Multiple-rod constructs have been proposed as a way to increase stability in long spinal fusion surgery compared to dual-rod constructs. In this biomechanical analysis of intact cadaveric thoracic spines, no differences in absolute overall stiffness or range of motion were found between dual-rod and multiple-rod constructs. Furthermore, no absolute differences in range of motion were observed at individual segments. However, multiple rod-constructs did exhibit more resistance to fatigue testing than dual-rod constructs. This work supports the current clinical work in the adult spinal deformity field showing reduced incidence of nonunion and rod breakage with multiple-rod constructs. Future biomechanical efforts should seek to explore the differences in constructs with longer duration fatigue testing, as the increased rigidity afforded by multiple-rod constructs may result in failure at the screw-bone interface.

Overall, multiple-rod constructs may play a beneficial role in affording additional stability during adult spinal deformity surgery with concomitant bony resections. This could ultimately lead to improved patient outcomes and fewer revision surgeries following adult spinal deformity surgery.

REFERENCES

1. Mahadevan V. Anatomy of the vertebral column. *Surgery (Oxford)* 2018;36:327–32.
2. Bazira PJ. Clinically applied anatomy of the vertebral column. *Surgery (Oxford)* 2021;39:315–23.
3. Liebsch C, Graf N, Appelt K, et al. The rib cage stabilizes the human thoracic spine: An in vitro study using stepwise reduction of rib cage structures. *PloS one* 2017;12:e0178733–e0178733.
4. Sham ML, Zander T, Rohlmann A, et al. Effects of the Rib Cage on Thoracic Spine Flexibility / Einfluss des Brustkorbs auf die Flexibilität der Brustwirbelsäule. 2005;50:361–5.
5. Yukawa Y, Kato F, Suda K, et al. Age-related changes in osseous anatomy, alignment, and range of motion of the cervical spine. Part I: Radiographic data from over 1,200 asymptomatic subjects. *Eur Spine J* 2012;21:1492–8.
6. Bernhardt M, Bridwell KH. Segmental analysis of the sagittal plane alignment of the normal thoracic and lumbar spines and thoracolumbar junction. *Spine (Philadelphia, Pa 1976)* 1989;14:717–21.
7. Hamill J, Knutzen K, Derrick TR. *Biomechanical basis of human movement*. 4th edition. Philadelphia: Wolters Kluwer Health; 2015.

8. Jaumard NV, Welch WC, Winkelstein BA. Spinal Facet Joint Biomechanics and Mechanotransduction in Normal, Injury and Degenerative Conditions. *J Biomech Eng* 2011;133:071010–071010.
9. Martin BI, Mirza SK, Spina N, et al. Trends in Lumbar Fusion Procedure Rates and Associated Hospital Costs for Degenerative Spinal Diseases in the United States, 2004 to 2015. *Spine (Philadelphia, Pa 1976)* 2019;44:369–76.
10. Raizman NM, O'Brien JR, Poehling-Monaghan KL, et al. Pseudarthrosis of the Spine. *Journal of the American Academy of Orthopaedic Surgeons* 2009;17:494–503.
11. MARTIN BI, MIRZA SK, COMSTOCK BA, et al. Reoperation rates following lumbar spine surgery and the influence of spinal fusion procedures. *Spine (Philadelphia, Pa 1976)* 2007;32:382–7.
12. BAGCHI K, MOHAIDEEN A, THOMSON JD, et al. Hardware complications in scoliosis surgery. *Pediatric radiology* 2002;32:465–75.
13. Koshimizu H, Nakashima H, Ohara T, et al. Implant-Related Complications after Spinal Fusion: A Multicenter Study. *Global spine journal* 2024;14:21925682221094267–81.
14. Soroceanu A, Diebo BG, Burton D, et al. Radiographical and Implant-Related Complications in Adult Spinal Deformity Surgery: Incidence, Patient Risk Factors, and Impact on Health-Related Quality of Life. *Spine (Philadelphia, Pa 1976)* 2015;40:1414–21.

15. Barton C, Noshchenko A, Patel V, et al. Risk factors for rod fracture after posterior correction of adult spinal deformity with osteotomy: a retrospective case-series. *Scoliosis* 2015;10:30–30.
16. Smith JS, Shaffrey CI, Ames CP, et al. Assessment of symptomatic rod fracture after posterior instrumented fusion for adult spinal deformity. *Neurosurgery* 2012;71:862–7.
17. Yang BP, Ondra SL, Chen LA, et al. Clinical and radiographic outcomes of thoracic and lumbar pedicle subtraction osteotomy for fixed sagittal imbalance. *Journal of neurosurgery Spine* 2006;5:9–17.
18. IKENAGA M, SHIKATA J, TAKEMOTO M, et al. Clinical outcomes and complications after pedicle subtraction osteotomy for correction of thoracolumbar kyphosis. *Journal of neurosurgery Spine* 2007;6:330–6.
19. Charosky S, Guigui P, Blamoutier A, et al. Complications and risk factors of primary adult scoliosis surgery: a multicenter study of 306 patients. *Spine (Philadelphia, Pa 1976)* 2012;37:693–700.
20. KOSTUIK JP, ERRICO TJ. Adult Idiopathic Scoliosis and Degenerative Scoliosis. Elsevier; 2009:307–42.
21. Dinizo M, Passias P, Kebaish K, et al. The Approach to Pseudarthrosis After Adult Spinal Deformity Surgery: Is a Multiple-Rod Construct Necessary? *Global spine journal* 2023;13:636–42.

22. Ohrt-Nissen S, Dahl B, Gehrchen M. Choice of Rods in Surgical Treatment of Adolescent Idiopathic Scoliosis: What Are the Clinical Implications of Biomechanical Properties? - A Review of the Literature. *Neurospine* 2018;15:123–30.
23. Yoshihara H MD, PhD. Rods in spinal surgery: a review of the literature. *The spine journal* 2013;13:1350–8.
24. PIENKOWSKI D, STEPHENS GC, DOERS TM, et al. Multicycle mechanical performance of titanium and stainless steel transpedicular spine implants. *Spine (Philadelphia, Pa 1976)* 1998;23:782–8.
25. STAMBOUGH JL, GENAIDY AM, HUSTON RL, et al. Biomechanical assessment of titanium and stainless steel posterior spinal constructs : Effects of absolute/relative loading and frequency on fatigue life and determination of failure modes. *Journal of spinal disorders* 1997;10:473–81.
26. Shah KN, Walker G, Koruprolu SC, et al. Biomechanical comparison between titanium and cobalt chromium rods used in a pedicle subtraction osteotomy model. *Orthopedic Reviews* 2018;10:7541–7541.
27. Nunn T, Varley E DO, Arunakul R MD, et al. 84. Cobalt Chromium Rods: How Do They Stack Up? *The spine journal* 2009;9:44S-44S.
28. Hellman MD MD, Haughom B MD, Wetters N MD, et al. Rod Fractures in Spinal Deformity Surgery: Does Cobalt Chrome Really Fracture Less Often? *The spine journal* 2013;13:S163–S163.

29. WEDEMEYER M, PARENT S, MAHAR A, et al. Titanium Versus stainless steel for anterior spinal fusions : An analysis of rod stress as a predictor of rod breakage during physiologic loading in a bovine model. *Spine (Philadelphia, Pa 1976)* 2007;32:42–8.
30. SCHEER JK, TANG JA, DEVIREN V, et al. Biomechanical analysis of cervicothoracic junction osteotomy in cadaveric model of ankylosing spondylitis: effect of rod material and diameter: Laboratory investigation. *Journal of neurosurgery Spine* 2011;14:330–5.
31. Cui Y, Lewis G, Qi G. Numerical Analysis of Models of the Standard TSRH Spinal Instrumentation: Effect of Rod Cross-sectional Shape. *Computer methods in biomechanics and biomedical engineering* 2002;5:75–80.
32. Banno T, Hasegawa T, Yamato Y, et al. Multi-Rod Constructs Can Increase the Incidence of Iliac Screw Loosening after Surgery for Adult Spinal Deformity. *Asian spine journal* 2019;13:500–10.
33. Rabinovich EP, Buell TJ, Wang TR, et al. Reduced occurrence of primary rod fracture after adult spinal deformity surgery with accessory supplemental rods: retrospective analysis of 114 patients with minimum 2-year follow-up. *Journal of neurosurgery Spine* 2021;35:504–12.
34. Lamas V, Charles YP, Tuzin N, et al. Comparison of degenerative lumbar scoliosis correction and risk for mechanical failure using posterior 2-rod instrumentation versus 4-rod instrumentation and interbody fusion. *Eur Spine J* 2021;30:1965–77.
35. Zhao J, Nie Z, Zhang Z, et al. Multiple-Rod Constructs in Adult Spinal Deformity Surgery: A Systematic Review and Meta-Analysis. *Asian Spine J* 2023;17:985–95.

36. Bourghli A, Boissière L, Kieser D, et al. Multiple-Rod Constructs Do Not Reduce Pseudarthrosis and Rod Fracture After Pedicle Subtraction Osteotomy for Adult Spinal Deformity Correction but Improve Quality of Life. *Neurospine* 2021;18:816–23.
37. Gehrchen M, Hallager DW, Dahl B, et al. Rod Strain After Pedicle Subtraction Osteotomy: A Biomechanical Study. *Spine (Philadelphia, Pa 1976)* 2016;41 Suppl 7:S24–S24.
38. Shen FH, Woods D, Miller M, et al. Use of the dual construct lowers rod strains in flexion-extension and lateral bending compared to two-rod and two-rod satellite constructs in a cadaveric spine corpectomy model. *The spine journal* 2021;21:2104–11.
39. Tan Q-C, Huang J-F, Bai H, et al. Effects of Revision Rod Position on Spinal Construct Stability in Lumbar Revision Surgery: A Finite Element Study. *Frontiers in bioengineering and biotechnology* 2022;9:799727–799727.
40. Scheer JK, Tang JA, Deviren V, et al. Biomechanical Analysis of Revision Strategies for Rod Fracture in Pedicle Subtraction Osteotomy. *Neurosurgery*;69. Available at https://journals.lww.com/neurosurgery/fulltext/2011/07000/biomechanical_analysis_of_revision_strategies_for.19.aspx. 2011.
41. Jager ZS MD, İnceoğlu S PhD, Palmer D BS, et al. Preventing Instrumentation Failure in Three-Column Spinal Osteotomy: Biomechanical Analysis of Rod Configuration. *Spine Deform* 2016;4:3–9.
42. Luca A, Ottardi C, Sasso M, et al. Instrumentation failure following pedicle subtraction osteotomy: the role of rod material, diameter, and multi-rod constructs. *European Spine Journal* 2017;26:764–70.

43. Seyed Vosoughi A, Joukar A, Kiapour A, et al. Optimal satellite rod constructs to mitigate rod failure following pedicle subtraction osteotomy (PSO): a finite element study. *The spine journal* 2019;19:931–41.
44. Park S-J, Lee C-S, Chang B-S, et al. Rod fracture and related factors after total en bloc spondylectomy. *The spine journal* 2019;19:1613–9.
45. Maccauro G, Spinelli MS, Mauro S, et al. Physiopathology of Spine Metastasis. *International Journal of Surgical Oncology* 2011;2011:107969–8.
46. Akazawa T, Kotani T, Sakuma T, et al. Rod fracture after long construct fusion for spinal deformity: clinical and radiographic risk factors. *J Orthop Sci* 2013;18:926–31.
47. Cadieux C. *Biomechanical Characterization of Semi-Rigid Constructs and the Potential Effect on Proximal Junctional Kyphosis in the Thoracic Spine*. The University of Western Ontario (Canada); 2022.
48. Kim YJ, Lenke LG. Thoracic pedicle screw placement: free-hand technique. *Neurology India* 2005;53:512–9.
49. Wilke HJ, Wenger K, Claes L. Testing criteria for spinal implants: recommendations for the standardization of in vitro stability testing of spinal implants. *European spine journal* 1998;7:148–54.
50. Shekouhi N, Vosoughi AS, Goel VK, et al. Does number of rods matter? 4-, 5-, and 6-rods across a lumbar pedicle subtraction osteotomy: a finite element analysis. *Spine Deform* 2023;11:535–43.

51. Hartmann S, Thomé C, Abramovic A, et al. The Effect of Rod Pattern, Outrigger, and Multiple Screw-Rod Constructs for Surgical Stabilization of the 3-Column Destabilized Cervical Spine - A Biomechanical Analysis and Introduction of a Novel Technique. *Neurospine* 2020;17:610–29.
52. Pereira B de A, Godzik J, Lehrman JN, et al. Pedicle Subtraction Osteotomy Construct Optimization: A Cadaveric Study of Various Multirod and Interbody Configurations. *Spine (Philadelphia, Pa 1976)* 2022;47:640–7.
53. Zhao J, Nie Z, Zhang Z, et al. Multiple-Rod Constructs in Adult Spinal Deformity Surgery: A Systematic Review and Meta-Analysis. *Asian Spine J* 2023;17:985–95.
54. Bridwell KH, Lenke LG, Cho SK, et al. Proximal junctional kyphosis in primary adult deformity surgery: evaluation of 20 degrees as a critical angle. *Neurosurgery* 2013;72:899–906.
55. Haldeman PB, Ward SR, Osorio J, et al. An evidence based conceptual framework for the multifactorial understanding of proximal junctional kyphosis. *Brain & spine* 2024;4:102807–102807.
56. Kim HJ, Iyer S. Proximal Junctional Kyphosis. *Journal of the American Academy of Orthopaedic Surgeons* 2016;24:318–26.
57. Lau D, Clark AJ, Scheer JK, et al. Proximal Junctional Kyphosis and Failure After Spinal Deformity Surgery: A Systematic Review of the Literature as a Background to Classification Development. *Spine (Philadelphia, Pa 1976)* 2014;39:2093–102.

58. KIM YJ, LENKE LG, BRIDWELL KH, et al. Proximal junctional kyphosis in adolescent idiopathic scoliosis after 3 different types of posterior segmental spinal instrumentation and fusions : Incidence and risk factor analysis of 410 cases. *Spine (Philadelphia, Pa 1976)* 2007;32:2731–8.
59. WATANABE K, LENKE LG, BRIDWELL KH, et al. Proximal Junctional Vertebral Fracture in Adults After Spinal Deformity Surgery Using Pedicle Screw Constructs: Analysis of Morphological Features. *Spine (Philadelphia, Pa 1976)* 2010;35:138–45.
60. Lopez Poncelas M, La Barbera L, Rawlinson J, et al. Proximal junctional failure after surgical instrumentation in adult spinal deformity: biomechanical assessment of proximal instrumentation stiffness. *Spine Deform* 2023;11:59–69.
61. Cazzulino A, Gandhi R, Woodard T, et al. Soft Landing technique as a possible prevention strategy for proximal junctional failure following adult spinal deformity surgery. *Journal of spine surgery (Hong Kong)* 2021;7:26–36.
62. Cadieux C, Brzozowski P, Fernandes RJR, et al. Topping-Off a Long Thoracic Stabilization With Semi-Rigid Constructs May Have Favorable Biomechanical Effects to Prevent Proximal Junctional Kyphosis: A Biomechanical Comparison. *Global spine journal* 2024;21925682241259695–21925682241259695.
63. Han SH MD, Hyun S-J MD, PhD, Kim K-J MD, PhD, et al. Rod stiffness as a risk factor for proximal junctional kyphosis after adult spinal deformity surgery: Comparative study between cobalt chrome multiple-rod constructs and titanium alloy two-rod constructs. *The spine journal* 2017;17:962–8.

64. Hyun S-J, Lenke LG, Kim Y-C, et al. Comparison of Standard 2-Rod Constructs to Multiple-Rod Constructs for Fixation Across 3-Column Spinal Osteotomies. *Spine (Philadelphia, Pa 1976)* 2014;39:1899–904.
65. Yamato Y, Hasegawa T, Togawa D, et al. Long additional rod constructs can reduce the incidence of rod fractures following 3-column osteotomy with pelvic fixation in short term. *Spine Deform* 2020;8:481–90.
66. Guevara-Villazón F, Boissiere L, Hayashi K, et al. Multiple-rod constructs in adult spinal deformity surgery for pelvic-fixated long instrumentations: an integral matched cohort analysis. *Eur Spine J* 2020;29:886–95.
67. Gupta S, Eksi MS, Ames CP, et al. A Novel 4-Rod Technique Offers Potential to Reduce Rod Breakage and Pseudarthrosis in Pedicle Subtraction Osteotomies for Adult Spinal Deformity Correction. *Operative neurosurgery (Hagerstown, Md)* 2018;14:449–56.
68. Moniz-Garcia D, Stoloff D, Akinduro O, et al. Two- versus multi-rod constructs for adult spinal deformity: A systematic review and Random-effects and Bayesian meta-analysis. *Journal of clinical neuroscience* 2023;107:9–15.
69. Ye J, Gupta S, Farooqi AS, et al. Use of multiple rods and proximal junctional kyphosis in adult spinal deformity surgery. *Journal of neurosurgery Spine* 2023;39:1–9.
70. Pennington Z, Cottrill E, Ahmed AK, et al. Paraspinal muscle size as an independent risk factor for proximal junctional kyphosis in patients undergoing thoracolumbar fusion. *Journal of neurosurgery Spine* 2019;31:380–8.

EDUCATION

Orthopaedic Surgery Residency

2021-Present

Chief Resident: Jun 2024 – Present

Junior Chief Resident: Jul 2022 – Jun 2024

Anticipated graduation: Jun 2026

Western University – London, ON

Master of Science, Surgery

2023 - Present

Thesis: *Stability of long multiple-rod constructs and dual-rod constructs in the thoracic spine: a biomechanical cadaveric study.*

Anticipated graduation: Aug 2024

Western University – London, ON

Doctor of Medicine

2017-2021

University of British Columbia – Vancouver, BC

Bachelor of Science, *cum laude*, Neuroscience

2012-2015

Brigham Young University – Provo, UT

PUBLICATIONS & PRESENTATIONS

Herrington BJ, Fernandes RR, Urquhart JC, Rampersaud YR, Bailey CS. Decompression and decompression and fusion and the influence of the lordosis distribution index (LDI) in the outcome of patients with degenerative lumbar spondylolisthesis (DLS). Canadian Spine Society Conference 2024 (podium).

Herrington BJ, Fernandes RR, Urquhart JC, Rampersaud YR, Bailey CS. Decompression, decompression and fusion, and the influence of lordosis distribution index on back pain in degenerative lumbar spondylolisthesis. Robert Zhong Department of Surgery Research Day, Western University, 2024 (poster).

Herrington BJ, Fernandes RR, Urquhart JC, Rasoulinejad P, Siddiqi F, Bailey CS. L3-L4 revision surgery after a reduction in the lordosis distribution index from initial L4-L5 fusion surgery. Residents' Research Day, Schulich School of Medicine & Dentistry, Western University, 2023 (podium).

Herrington BJ, Fernandes RR, Urquhart JC, Rasoulinejad P, Siddiqi F, Bailey CS. L3-L4 Hyperlordosis and Decreased Lower Lumbar Lordosis Following Short-Segment L4-L5 Lumbar Fusion Surgery is Associated With L3-L4 Revision Surgery for Adjacent Segment Stenosis. *Global Spine Journal*. 2023;0(0). doi:[10.1177/21925682231191414](https://doi.org/10.1177/21925682231191414)

Herrington BJ, Fernandes RR, Urquhart JC, Rasoulinejad P, Fawaz S, Bailey CS. L3-4 hyperlordosis after a reduction in lower lumbar lordosis with L4-L5 fusion surgery is common in patients requiring L3-4 revision surgery for adjacent segment disease. Canadian Spine Society Conference 2023 (podium).

Herrington BJ, Fernandes RR, Urquhart JC, Bailey CS. Adjacent segment disease after a reduction of the lower lumbar lordosis angle in spine fusion surgery. Residents' Research Day, Schulich School of Medicine & Dentistry, Western University, Oct 18, 2022 (poster).

Sawatzky B, **Herrington BJ**, Choi K, Mortensen WB, Borisoff J, Sparrey C, Laskin JJ. Acute physiological comparison of sub-maximal exercise on a novel adapted rowing machine and arm crank ergometry in people with a spinal cord injury. *Spinal Cord* 60, 694–700 (2022). <https://doi.org/10.1038/s41393-022-00757-2>

Herrington BJ, Vikulova D, Bitoiu B, Lynch K, Brown C, Ng P, Pimstone SN, Brunham LR. Elevated lipoprotein (a) correlates with increased atherosclerotic disease severity in a very premature coronary artery disease cohort. Heart and Lung Health Fest 2019 (poster).

Herrington BJ, Barzee B, Barlow S, Robison S, Hansen M, Salin A, Stone M, Bridgewater J, Kavafyan T, Steed K, Stark ME, Dong H, Toga AW, Vinters HV, Wisco JJ. The spatial relationship between iron, tangles, and plaques in the subiculum. Society for Neuroscience (SFN). Abstr 2014 (poster).

Barlow SH, Hansen M, Salin A, Barzee B, Steed K, Wisco JJ, Stone, M, Bridgewater J, Kavafyan T, Stark ME, Vinters HV, Dong H, Toga AW, **Herrington BJ**. Spatial correlation between iron, plaques, and tangles in the entorhinal cortex may present iron to be a potential biomarker for Alzheimer's disease using MRI. Society for Neuroscience (SFN). Abstr 2014 (poster).

ACADEMIC LECTURES

Herrington BJ, King G., Ladd A. Basilar Thumb Arthritis. Western Orthopaedic Surgery Academic Day. May 2024.

Herrington BJ, Singh S. Spinopelvic Dissociation. Western Orthopaedic Surgery Department Grand Rounds. Mar 2024.

Herrington BJ, Pollock J, Litchfield R. Rotator Cuff Injuries. Western Orthopaedic Surgery Resident Academic Day. Jan 2024.

Herrington BJ, Lawendy A. Multiple Gunshot Wound Injuries. Western Orthopaedic Surgery Department Grand Rounds. Oct 2023.

Herrington BJ, Giffin R. Iatrogenic nerve injuries after peripheral nerve blocks. Western Orthopaedic Surgery Department Grand Rounds. Apr 2023.

Herrington BJ, MacDonald S. Revision Total Knee Arthroplasty. Western Orthopaedic Surgery Resident Academic Day. Feb 2023.

Herrington BJ, Lebel M. Scapula, acromioclavicular joint, clavicle, and sternoclavicular joint trauma. Western Orthopaedic Surgery Resident Academic Day. Jun 2023.

Herrington BJ. Current Management of Rib Fractures. Critical Care Department Grand Rounds. Nov 2022.

Herrington BJ. Heterotopic Ossification: Diagnosis and Management. Physical Medicine and Rehabilitation Resident Academic Rounds. Sep 2022.

Herrington BJ. Nonoperative Treatments in Spine Surgery. Physical Medicine and Rehabilitation Resident Academic Rounds. Jul 2022.

RESEARCH EXPERIENCE

Western University Combined Neurosurgical and Orthopaedic Spine Program

2021-Present

Western University – London, ON

Role: Resident Physician Researcher

Principal Investigator: Dr. Chris S. Bailey

International Collaboration on Repair Discoveries (ICORD) University of British Columbia – Vancouver, B.C. Role: Medical Student Principal Investigators: Dr. Bonita Sawatzky and Dr. James Laskin	2020-2021
Centre for Heart & Lung Innovation University of British Columbia – Vancouver, B.C. Role: Medical Student Principal Investigator: Dr. Liam Brunham	2018-2019
Department of Pathology University of Utah – Salt Lake City, UT Role: Visiting Scholar Principal Investigator: Dr. June Round	2018
Alzheimer’s Disease Research Laboratory Brigham Young University – Provo, UT Role: Undergraduate Student Principal Investigator: Dr. Jonathan Wisco	2013-2015
Nitric Oxide Laboratory University of British Columbia – Vancouver, B.C. Role: Research Assistant Principal Investigator: Dr. Chris Miller	2013 & 2014

PROFESSIONAL EXPERIENCE

London Health Sciences Centre London, ON Orthopaedic Surgery Resident Physician	2021-Present
Ultradent Products, Inc. South Jordan, UT Quality Control Microbiologist	2015-2017
Frontline Pest Professionals Manassas, VA Salesperson	2015
Department of Clinical Psychology – Brigham Young University Provo, UT Office Specialist	2014-2015
Lifebank Corp. – Cord Blood Bank Burnaby, B.C. Laboratory Specialist	2011

CERTIFICATIONS

• United States Medical Licensing Examination Step 3	Dec 2023
• Advanced Trauma Life Support – American College of Surgeons	Jun 2021
• Medical Council of Canada Qualifying Examination MCCQE	Apr 2021
• United States Medical Licensing Examination Step 2	July 2020
• Advanced Cardiovascular Life Support - <i>Heart & Stroke Foundation</i>	Jan 2020
• Basic Life Support - <i>Heart & Stroke Foundation</i>	Oct 2019
• United States Medical Licensing Examination Step 1	May 2019

AWARDS

- Resident Research Travel Grant – *Western University – London, ON* **2024**
- Most Outstanding Resident Teacher – *Western University – London, ON* **2023-2024**
- Resident Research Travel Grant – *Western University – London, ON* **2023**
- James H. Roth award for best resident poster presentation – *Western University – London, ON* **2022**
- *cum laude* – *Brigham Young University – Provo, UT* **2015**
- ORCA Research Grant – *Brigham Young University – Provo, UT* **2014 & 2015**
- Academic Scholarship – *Brigham Young University – Provo, UT* **2013-2015**
- Queen’s Venturer Award – *Scouts Canada – Victoria, B.C.* **2009**

MEMBERSHIPS

- Canadian Spine Society **2022-Present**
- North American Spine Society **2021-Present**
- American Academy of Orthopaedic Surgeons **2021-Present**
- Ontario Medical Association **2021-Present**
- Canadian Medical Association **2017-Present**
- Society for Neuroscience **2014-2022**
- College of Physicians & Surgeons of British Columbia **2017-2021**
- Medical Undergraduate Society – University of British Columbia **2017-2021**